Environmental Pollution 286 (2021) 117309

Contents lists available at ScienceDirect

Environmental Pollution

journal homepage: www.elsevier.com/locate/envpol

Nitrogen burden from atmospheric deposition in East Asian oceans in 2010 based on high-resolution regional numerical modeling☆

Syuichi Itahashi [a,*], Kentaro Hayashi [b], Shigenobu Takeda [c], Yu Umezawa [d], Kazuhide Matsuda [d], Tatsuya Sakurai [e], Itsushi Uno [f]

[a] Environmental Science Research Laboratory, Central Research Institute of Electric Power Industry (CRIEPI), 1646 Abiko, Abiko, Chiba, 270-1194, Japan
[b] Institute for Agro-Environmental Sciences, National Agriculture and Food Research Organization, 3-1-3, Kannondai, Tsukuba, Ibaraki, 305–8604, Japan
[c] Graduate School of Fisheries and Environmental Sciences, Nagasaki University, 1-14 Bunkyomachi, Nagasaki, Nagasaki, 852-8521, Japan
[d] Faculty of Agriculture, Tokyo University of Agriculture and Technology, 3-5-8 Saiwai-cho, Fuchu, Tokyo, 183-8509, Japan
[e] School of Science Ane Engeneering, Meisei University, 2-1 Hodokubo, Hino, Tokyo, 191-8506, Japan
[f] Research Institute for Applied Mechanics (RIAM), Kyushu University, 6-1 Kasuga Park, Kasuga, Fukuoka, 816-8580, Japan

ARTICLE INFO

Keywords:
Nitrogen deposition
Atmospheric dry deposition
Atmospheric wet deposition
East China Sea
Regional chemical transport model

ABSTRACT

East Asian oceans are possibly affected by a high nitrogen (N) burden because of the intense anthropogenic emissions in this region. Based on high-resolution regional chemical transport modeling with horizontal grid scales of 36 and 12 km, we investigated the N burden into East Asian oceans via atmospheric deposition in 2010. We found a high N burden of 2–9 kg N ha^{-1} yr^{-1} over the Yellow Sea, East China Sea (ECS), and Sea of Japan. Emissions over East Asia were dominated by ammonia (NH_3) over land and nitrogen oxides (NO_x) over oceans, and N deposition was dominated by reduced N over most land and open ocean, whereas it was dominated by oxidized N over marginal seas and desert areas. The verified numerical modeling identified that the following processes were quantitatively important over East Asian oceans: the dry deposition of nitric acid (HNO_3), NH_3, and coarse-mode (aerodynamic diameter greater than 2.5 μm) NO_3^-, and wet deposition of fine-mode (aerodynamic diameter less than 2.5 μm) NO_3^- and NH_4^+. The relative importance of the dry deposition of coarse-mode NO_3^- was higher over open ocean. The estimated N deposition to the whole ECS was 390 Gg N yr^{-1}; this is comparable to the discharge from the Yangtze River to the ECS, indicating the significant contribution of atmospheric deposition. Based on the high-resolution modeling over the ECS, a tendency of high deposition in the western ECS and low deposition in the eastern ECS was found, and a variety of deposition processes were estimated. The dry deposition of coarse-mode NO_3^- and wet deposition of fine-mode NH_4^+ were the main factors, and the wet deposition of fine-mode NO_3^- over the northeastern ECS and wet deposition of coarse-mode NO_3^- over the southeastern ECS were also found to be significant processes determining N deposition over the ECS.

1. Introduction

The central pathway for the supply of nutrients to the ocean surface layer is biological nitrogen fixation (Shiozaki et al., 2010; Fowler et al., 2013). In addition to this pathway, nutrients originating from the atmosphere via deposition processes are also important for the supply to the ocean surface layer, and the supply of such nutrients has steadily increased since 2000, particularly over Asia, owing to the increase of anthropogenic emissions (Galloway et al., 2004; Duce et al., 2008; Kim et al., 2011; Kim et al., 2014; Jickells et al., 2017; GESAMP, 2018). The emission of nitrogen oxide (NO_x), defined as the sum of nitrogen oxide (NO) and nitrogen dioxide (NO_2), from anthropogenic sources (e.g., industry, power plants, transportation, domestic) produces nitric acid (HNO_3) and various other nitrogen (N) compounds through atmospheric photochemistry. The amount of NO_x emissions in China increased threefold from 1980 to 2000 (Ohara et al., 2007), doubled from 2000 to 2010 (Kurokawa et al., 2013; Itahashi et al., 2014), and reached its peak in 2011 and subsequently declined (Irie et al., 2016; Itahashi et al.,

☆ This paper has been recommended for acceptance by Jörg Rinklebe.

* Corresponding author. Environmental Science Research Laboratory, Central Research Institute of Electric Power Industry (CRIEPI), 1646 Abiko, Abiko, Chiba, 270–1194, Japan.
E-mail addresses: isyuichi@criepi.denken.or.jp (S. Itahashi), kentaroh@affrc.go.jp (K. Hayashi), s-takeda@nagasaki-u.ac.jp (S. Takeda), umezawa@me.tuat.ac.jp (Y. Umezawa), kmatsuda@cc.tuat.ac.jp (K. Matsuda), tatsuya.sakurai@meisei-u.ac.jp (T. Sakurai), uno@riam.kyushu-u.ac.jp (I. Uno).

https://doi.org/10.1016/j.envpol.2021.117309
Received 30 January 2021; Received in revised form 6 April 2021; Accepted 1 May 2021
Available online 5 May 2021

2019; Kurokawa and Ohara, 2020). The concentration of ammonia (NH_3), a highly reactive gas that is mainly emitted from agricultural sources (livestock and fertilizer), is also remarkably high over East Asia (Kong et al., 2020; Wang et al., 2020). This gas plays an important role in the formation of nitrate (NO_3^-) and ammonium (NH_4^+) aerosol in this region (hereinafter referred to as pNO_3^- and pNH_4^+, respectively, to specify that it is particulate matter rather than dissolved ions).

Continuous increases in atmospheric N deposition, which provide N as a nutrient, can cause eutrophication. Seas in East Asia face a high risk of eutrophication due to land-based N loads from the surrounding countries (IOC-UNESCO and UNEP, 2016; Gonzales et al., 2019). An ongoing international project, the International Nitrogen Management System (INMS), focuses on the East China Sea (ECS) as part of the "East Asia Regional Demonstration" (INMS , 2020; 2021). Land-based N loads roughly consist of riverine exports and atmospheric deposition. Detailed information of N deposition over the ECS is indispensable for assessing its N pollution status. Based on budget analyses, it was estimated that the nitrate influx to the ECS from the atmosphere was more than 30% of the influx from river discharge (Chen and Wang, 1999). Additionally, the annual atmospheric influx of nitrate to the ECS was shown to correspond to 60% of the river discharge from the Yangtze River based on onboard observations during cruises by the research vessel Hakuho Maru (Nakamura et al., 2005). Using a tracking technique, Zhang et al. (2019) evaluated differences in contributions of N to the inner, middle, and outer shelves of the ECS by four external nutrient sources, namely, the Kuroshio Current, the Taiwan Strait, rivers, and the atmosphere, and found that atmospheric inputs contributed more than 20% of N supply over the inner shelf (depth, 0–50 m) and middle shelf (depth, 50–100 m). It was also reported that the importance of the atmospheric supply of N was greater than or equal to the riverine input over the Yellow Sea (YS) (Zhang and Lui, 1994) and over the shelf of the ECS (Zhang et al., 2007). These studies demonstrated the importance of atmospheric N deposition in East Asian oceans. It has also been shown that atmospheric N inputs affect oceanic primary production (Onitsuka et al., 2009; Taketani et al., 2018). In our previous study, the deposition of total nitrate (defined as the sum of pNO_3^- and HNO_3) over East Asian marginal seas was estimated using a regional chemical transport model (Uno et al., 2007). Additionally, we later expanded upon this study by including the interactions between HNO_3 and sea salt to produce coarse-mode pNO_3^- (Itahashi et al., 2016). The analyzed periods were 1980–2003 and 2002–2004, respectively, on the way of the increase in emissions in East Asia, especially for NO_x (Li et al., 2017; Kurokawa and Ohara, 2020). The purpose of the present study is to extend the analysis period of the N burden from atmospheric deposition over East Asian oceans, which are considered to have a high risk of N burden because the N emission status has been dramatically changing in this region. This paper is structured as follows. In Section 2, the framework of the model analysis and the modeling design are described, and observations for evaluating the modeling performance and its protocols are provided. In Section 3, an evaluation of the modeling performance is presented, the analysis of the N burden over East Asian oceans is discussed, and a detailed analysis over the ECS is presented based on the high-resolution simulation. Finally, in Section 4, conclusions and potential directions for future study are presented.

2. Materials and methods

2.1. Framework of model analysis

In this study, we estimated the N burden from the atmosphere to the ocean in East Asia in 2010. NO_x emissions in China had increased up to 2011, whereas sulfur dioxide (SO_2) emissions have decreased since 2005 (Kurokawa and Ohara, 2020). As a result of these changes in NO_x and SO_2 emissions, the chemical composition over East Asia has become N-rich in both the atmosphere (Itahashi et al., 2017; Wang et al., 2017; Uno et al., 2020) and precipitation (Itahashi et al., 2015; Itahashi et al., 2018a). Therefore, it might be expected that N deposition into the adjacent East Asian oceans has also increased. The year 2010 was targeted in the harmonization of multi-scale and multi-model activities (Galmarini et al., 2017), and a high-spatial-resolution emission inventory with a 0.1 ° × 0.1 ° grid over the whole world is available (Janssens-Maenhout et al., 2015). This year was also the target period of the Model-Intercomparison Study in Asia (MICS-Asia) phase III (Chen et al., 2019; Ge et al., 2020; Itahashi et al., 2020a; Kong et al., 2020); however, its horizontal spatial resolution was 45 km to cover the whole of Asia, and ocean regions are not extensively focused on. The present study used a higher spatial resolution of 36 km over East Asia and was nested to a spatial resolution of 12 km over a rectangular region surrounding the ECS as a target area. Additionally, in our previous study, although coarse-mode pNO_3^- was incorporated via reaction with sea-salt, mineral dust was not considered. In MICS-Asia III, the implementation of a dust scheme was noted as being key to improving the modeling performance for particulate matter with aerodynamic diameters of less than 10 μm (PM_{10}) (Tan et al., 2020). Thus, in the present study, a dust scheme was implemented and the N burdens with and without this scheme were compared. Using this regional modeling design, this study elucidates the N burden due to atmospheric deposition over East Asian oceans. A schematic representation of N deposition from the atmosphere is shown in Fig. 1.

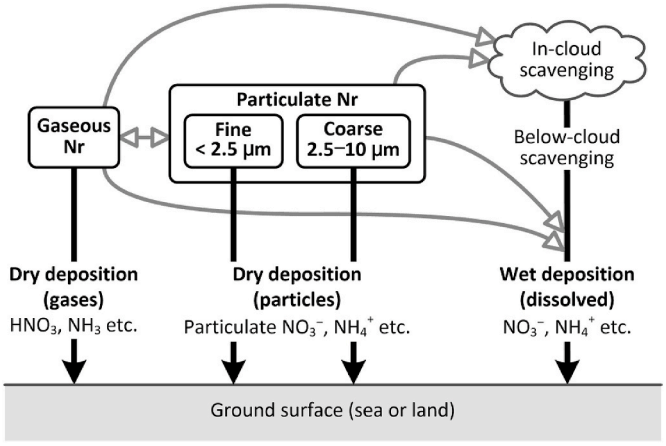

Fig. 1. Schematic view of nitrogen (N) deposition processes. Nr, reactive nitrogen; HNO_3, nitric acid; NH_3, ammonia; NO_3^-, nitrate; NH_4^+, ammonium. Other Nr chemical species were also treated in the modeling analysis (see the main text for details).

2.2. Design of chemical transport model

The Community Multiscale Air Quality (CMAQ) model version 5.2.1 was applied as the chemical transport model in this study (U.S. EPA, 2018). The simulation domain covered the whole of East Asia with a horizontal grid resolution of 36 km and was nested over the ECS with a horizontal grid resolution of 12 km (see Fig. 2 for the locations of these domains). In the vertical layer configuration, 44 nonuniform layers from the surface to 50 hPa were set to fully represent the stratosphere-to-troposphere transport (Mathur et al., 2017; Itahashi et al., 2020b). To drive the CMAQ, the meteorological fields were simulated by the Weather Research and Forecasting (WRF) model version 3.6.1 (Skamarock et al., 2008). The WRF used a MODIS-based land-use dataset with 21 categories, including lake. The detailed configuration of the WRF is the same as in our previous study, which conducted precipitation analysis over East Asia (Itahashi et al., 2015). As input data for the CMAQ, the emission dataset was created as follows: anthropogenic emissions from the high-spatial-resolution global emission inventory developed for the Hemispheric Transport of Air Pollution (HTAP) version 2.2 (Janssens-Maenhout et al., 2015); biogenic

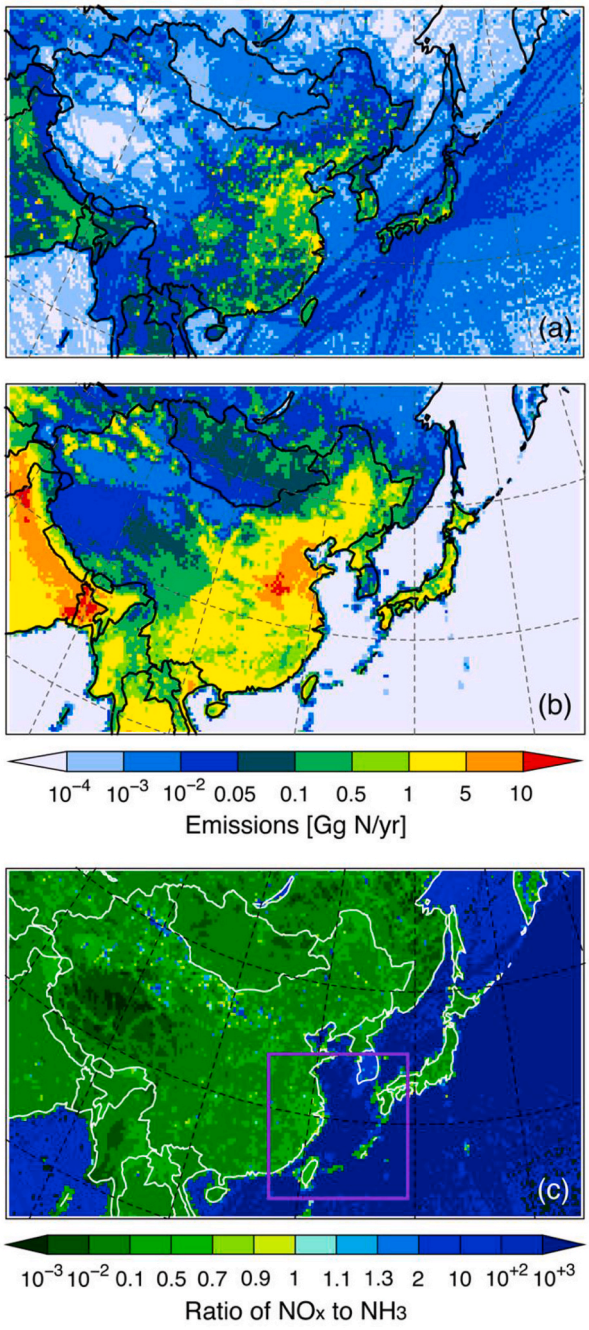

Fig. 2. Maps of the emissions of (a) NO_x and (b) NH_3 used in this study. (c) The ratio between emissions of NO_x and NH_3; values greater than unity (blue colors) indicate an NO_x-rich emission status, and values less than unity (green colors) indicate an NH_3-rich emission status. The purple rectangle indicates the nested domain for detailed analysis over the East China Sea.

emissions from the Model of Emissions of Gases and Aerosols from Nature (MEGAN) (Guenther et al., 2012); biomass burning emissions from the Global Fire Emissions Database (GFED) version 4.1 (van der Werf et al., 2017); and emissions from 15 active volcanoes in Japan from observational data obtained by the Japan Meteorological Agency (JMA, 2020). The emissions of NO_x and NH_3 used in this study are illustrated in Fig. 2(a) and (b). From the viewpoint of emissions, land is dominated by NH_3 and ocean is dominated by NO_x. The initial and lateral boundary conditions for chemical species were taken from the global model of the Model for Ozone and Related Chemical Tracers (MOZART) version 4 (Emmons et al., 2010). The WRF and CMAQ simulations covered the

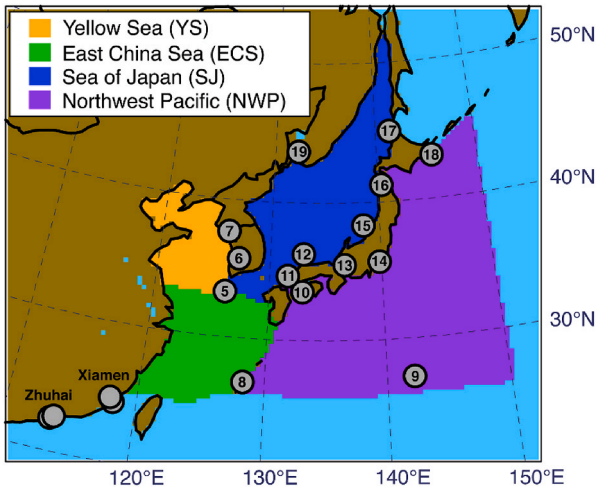

Fig. 3. The analyzed areas over marginal seas (Yellow Sea; YS, East China Sea; ECS, and Sea of Japan; SJ) and open ocean (Northwest Pacific; NWP) in East Asia. Gray circles indicate observation sites of the Acid Deposition Monitoring Network in East Asia (EANET), and the numbers correspond to Table 1.

period from December 1, 2009 to December 31, 2010, with the one month of December 2009 being discarded as a spin-up period.

Gas and aerosol chemistry in the CMAQ were respectively adopted for SAPRC07 (Hutzell et al., 2011) and aero 6 with non-volatile primary organic aerosol (Simon and Bhave, 2012). To improve the modeling performance for sulfate (SO_4^{2-}) during winter, aqueous-phase production was enhanced based on our previous studies (Itahashi et al., 2018b, 2018c). In order to simulate coarse-mode pNO_3^- and hence the partitioning between the gas- and aerosol phase and the size distribution of pNO_3^-, sea salt and dust aerosols are important factors (Uematsu et al., 2003; Itahashi et al., 2016; Uno et al., 2017a, 2017b, 2017c). The updated scheme for sea salt emissions in CMAQ (Gantt et al., 2015) and the newly developed dust scheme for CMAQ were adopted (Foroutan et al., 2017). Because the Noah land surface model was used in this study, the calculated soil moisture was multiplied by a factor of 0.1 to avoid the suppression of dust emission (Darmenova et al., 2009). Because of the implementation of the dust scheme, metallic ions related to mineral dust affect the gas and aerosol partitioning via ISORROPIA thermodynamics (Karydis et al., 2016). The dry and wet deposition schemes in the CMAQ model were used; these are respectively described in Pleim et al. (2001) and Fahey et al. (2017). The analyzed chemical species of reactive nitrogen (Nr, i.e., N species other than molecular N) were oxidized N of pNO_3^-, NO, NO_2, nitrogen trioxide (NO_3), nitrous acid (HNO_2), HNO_3, peroxynitric acid (HNO_4), dinitrogen pentoxide (N_2O_5), peroxyacetyl nitrate (PAN), and related species (hereafter referred to as PANs), chlorine-related N (e.g., Sarwar et al., 2012; Sarwar et al., 2014), nitrophenols, organic nitrates (e.g., Pye et al., 2015; Mathur et al., 2017), and reduced N of pNH_4^+ and NH_3. The simulated hourly average concentration, and the information of the aerosol distributions were used to calculate fine- and coarse-mode (divided by 2.5 μm) aerosols. The analyzed areas as East Asian Oceans are shown in Fig. 3 following the definitions of the International Hydrographic Organization (IHO). In this study, the YS, ECS, and Sea of Japan (SJ) are defined as marginal seas, and the Northwest Pacific (NWP) is defined as open ocean.

2.3. *Observations for the evaluation of modeling performance and its protocol*

The observational data for the ambient concentration and wet deposition over East Asia were obtained from the Acid Deposition Monitoring Network in East Asia (EANET) (EANET, 2020). Since the year 2000, EANET observations have been continuously providing the

Table 1
Information of the observation sites of the Acid Deposition Monitoring Network in East Asia (EANET) that were used for the evaluation of ambient concentration and wet deposition.

No.	Country	Site name	Latitude (°)	Longitude (°E)	Altitude (m a.s.l.)	Automatic monitor	Filter pack	Wet deposition
	China	Zhuhai						
1		- Zhuxiandong	22.20	113.52	18			✓
2		- Xiang Zhou Xiamen	22.27	113.57	29		✓	✓
3		- Hongwen	24.47	118.13	39	✓	✓	✓
4		- Xiaoping	24.85	118.03	530			✓
5	Republic of Korea	Cheju	33.30	126.16	37	✓	✓	✓
6		Imsil	35.60	127.18	217	✓	✓	✓
7		Kanghwha	37.70	126.28	60	✓	✓	✓
8	Japan	Hedo	26.87	128.25	60	✓	✓	✓
9		Ogasawara	27.09	142.22	212	✓	✓	✓
10		Yusuhara	33.38	132.93	790	✓	✓	✓
11		Banryu	34.68	131.80	53	✓	✓	✓
12		Oki	36.29	133.19	90	✓	✓	✓
13		Ijira	35.57	136.69	140	✓	✓	✓
14		Tokyo	35.69	139.76	26		✓	✓
15		Sadoseki	38.25	138.40	129	✓	✓	✓
16		Tappi	41.25	140.35	106	✓	✓	✓
17		Rishiri	45.12	141.21	40	✓	✓	✓
18		Ochiishi	43.16	145.50	49	✓	✓	✓
19	Russia	Primorskaya	43.70	132.12	85		✓	✓

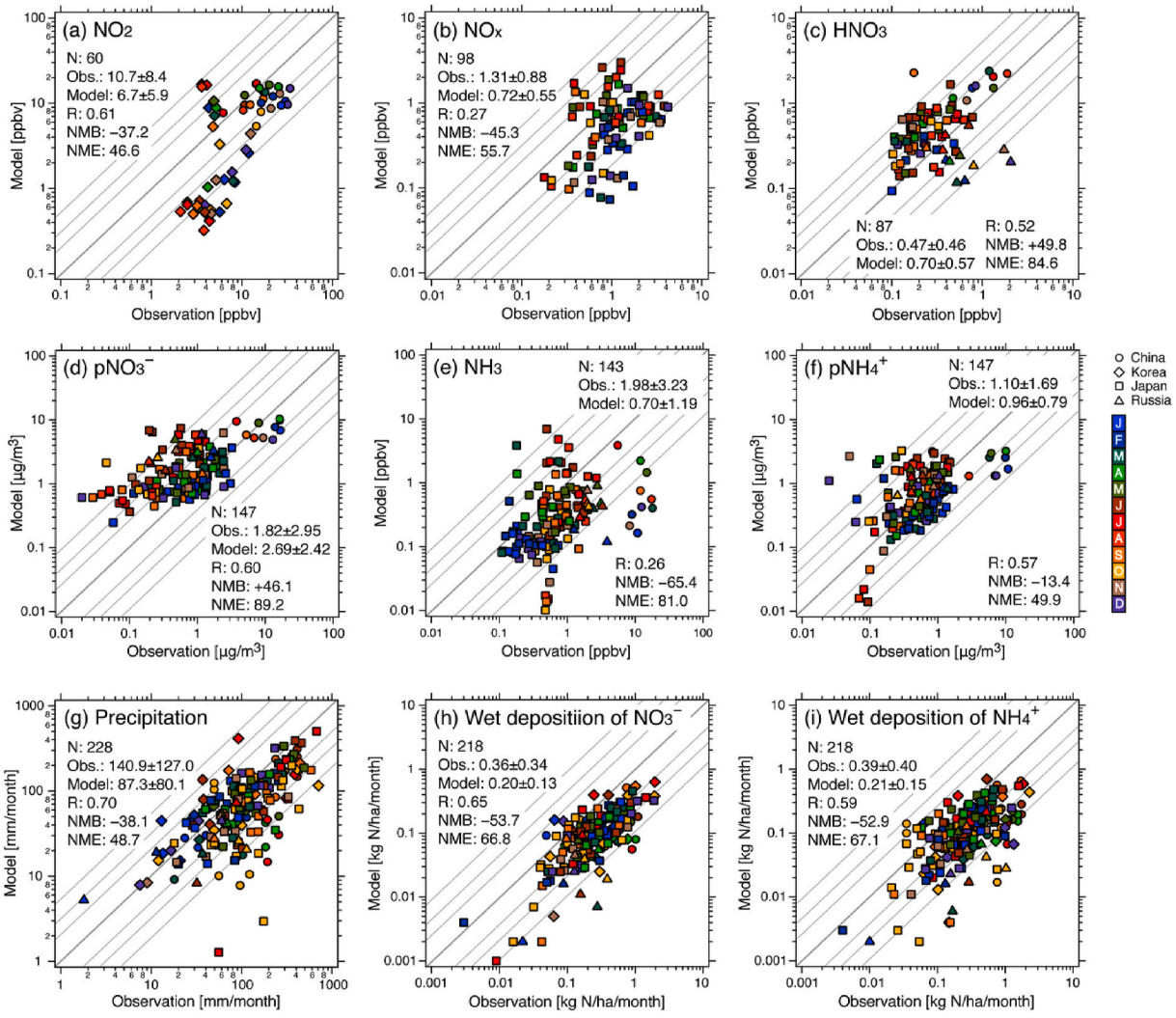

Fig. 4. Scatter plots between EANET observations and model simulations for ambient concentrations of NO_2, NO_x, HNO_3, pNO_3^-, NH_3, and pNH_4^+ and the wet deposition of NO_3^- and NH_4^+ on a monthly time-scale. Different symbols denote countries and different colors denote months in 2010.

ambient concentration and wet deposition over Asia (e.g., Endo et al., 2011; Ban et al., 2016). From EANET data, observation sites located along coastlines were used. These sites are also mapped in Fig. 3 and their details are listed in Table 1. Automatic gas monitoring was conducted using the chemiluminescence detection method; NO_2 was available for China and the Republic of Korea, and NO_X was available for Japan with a temporal resolution of 1 h. Based on the four-stage filter pack method, pNO_3^- and pNH_4^+ in total suspended particle (TSP) and HNO_3 and NH_3 gases were measured daily for the Republic of Korea and every two weeks for China and Japan (EANET, 2010a). The sum of the fine- and coarse-mode concentrations of pNO_3^- and pNH_4^+ simulated by the model were compared for the measured pNO_3^- and pNH_4^+ in TSP. For ambient concentrations, months with less than 60% complete data were discarded in the comparisons according to the guidelines of the Japan Environmental Laboratories Association (JELA (2020), and monthly-averaged values were used for model validation. Based on this criterion, the observed data at sites in the Republic of Korea (site nos. 5, 6, and 7) were discarded. Wet deposition was measured by a wet-only sampler designed to collect precipitation samples during rainfall and was analyzed by ion chromatography (EANET, 2010b), except for Primorskaya (site no. 19). At Primorskaya, spectrophotometry was used to analyze the wet deposition components. For wet deposition, data completeness was checked using the duration of precipitation coverage and the total precipitation amount; the data discarded by EANET were not used for comparison. Monthly-accumulated wet deposition data were used for model evaluation. The observational data used in this study are available from the EANET data report (EANET, 2020), and details are also included in EANET (2012).

The information of the size-resolved aerosol concentration was not available from EANET observations; however, this information is important because of the different roles of fine- and coarse-mode aerosols for deposition processes (Itahashi et al., 2016). In 2010, the training ship Nagasaki Maru conducted observations for the fine- and coarse-mode (divided by 2.5 μm) aerosol concentration during a cruise from April to December around the eastern ECS. Sampling was conducted on a Teflon filter with a high-volume virtual impactor air sampler (AS-9, Kimoto Electric Co. Ltd., Japan) on the compass deck of the Nagasaki Maru, and concentrations of water-soluble inorganic N were analyzed by standard colorimetric techniques using an autoanalyzer (AACS 4; BLTEC, Japan) (Yamada et al., 2013). Measurements with an accumulative flow below 60 m^3 during each sampling period were not used for this analysis due to the insufficient measurement volume. A total of 62 samples were available.

To evaluate the modeling performance, the correlation coefficient (R), normalized mean bias (NMB), and normalized mean error (NME) were used. The NMB and NME are defined according to the following formulae:

$$\mathrm{NMB} = \frac{\sum_1^N (M_i - O_i)}{\sum_1^N O_i} \quad (1)$$

$$\mathrm{NME} = \frac{\sum_1^N |M_i - O_i|}{\sum_1^N O_i} \quad (2)$$

where N is the total number of paired observations (O) and models (M). Recommendations for the modeling performance for the ambient concentration of $PM_{2.5}$ and its components were proposed by Emery et al. (2017). For daily pNO_3^-, R was not used to determine the model performance, the goals (i.e., for the best model performance) were NMB $<$ $\pm$15% and NME $<$ +65%, and the criteria (i.e., for an acceptable model performance) were NMB $<$ $\pm$65% and NME $<$ +115%. For the daily pNH_4^+, the goals were R $>$ 0.70, NMB $<$ $\pm$10%, and NME $<$ +35% and the criteria were R $>$ 0.40, NMB $<$ $\pm$30%, and NME $<$ +50%. These scores were set based on a literature review of modeling studies conducted over the U.S. and on the daily-averaged aerosol concentration. Because of the lack of indexes to evaluate the modeling performance, we used the above values to judge the modeling performance in this study.

3. Results and discussion

3.1. Evaluation of modeling performance over East Asian oceans

Before the discussion of the N burden over East Asian oceans, the modeling performance for the ambient concentration and wet deposition over East Asia was evaluated using monthly EANET observations (EANET, 2020). Fig. 4 shows a scatter plot between observed and modeled values with statistical scores for the ambient concentrations of NO_2, NO_x, HNO_3, pNO_3^-, NH_3, and pNH_4^+. For the NO_2 concentrations over China and Korea (Fig. 4(a)), the model showed underestimation, while for the NO_x concentrations over Japan (Fig. 4(b)), the model also showed underestimation. For HNO_3 (Fig. 4(c)), the model showed positive bias. For the analysis without the dust scheme, a tendency of overestimation was found for HNO_3, which was improved by including the chemical reactions with mineral dust components (Supplementary Information) because HNO_3 was consumed by mineral dust components to produce coarse-mode pNO_3^-. This shows the importance of the dust scheme for improving model performance and for the subsequent estimation of deposition. For pNO_3^- (Fig. 4(d)), the model showed overestimation, especially during summer; however, the NMB and NME were within the performance criteria. For NH_3 (Fig. 4(e)), the model had difficulty capturing the observed features compared to other N species. Data with a higher temporal resolution are required for NH_3 as its ambient concentrations fluctuate to a large degree, even within a single season (e.g., Sakurai et al., 2018). For pNH_4^+ (Fig. 4(f)), the modeling performance judged by R, NMB, and NME satisfied the criteria. In terms of the observational uncertainties, the filter pack method used in EANET is known to introduce artifacts for the volatile component of ammonium nitrate (NH_4NO_3) (Seinfeld and Pandis, 2016). These artifacts are affected by temperature and lead to the overestimation of concentrations of the gases HNO_3 and NH_3 and the underestimation of pNO_3^- and pNH_4^+, especially in summer. The discrepancy between the observed and modeled values in summer (red colors in Fig. 4) are partly due to the observational artifacts. In addition to the judgment based on the recommended criteria, the modeling performance achieved in this study was compared to those of other studies. The modeling performance for NO_2 and NH_3 was comparable to that reported in MICS-Asia (Kong et al., 2020), and the performance for pNO_3^- and pNH_4^+ was also comparable to that reported in MICS-Asia (Chen et al., 2019). The concentration of NO_x was underestimated during winter, which was similar to the results of a model inter-comparison study in Japan by Yamaji et al. (2020). Overall, the model performed well for capturing the observed ambient concentration. The modeling performance for the total aerosol concentration (PM_{10} and aerosol optical depth) was improved by the dust scheme (Supplementary Information). Based on these evaluations for ambient concentration, we expect that dry deposition can be simulated but also consider that the observational uncertainties, especially for dry deposition velocities, should be considered in future work (e.g., Baker et al., 2017).

Scatter plots between the observed and modeled wet deposition are shown in Fig. 4. Precipitation (Fig. 4(g)) and the wet deposition of NO_3^- (Fig. 4(h)) and NH_4^+ (Fig. 4(i)) were underestimated in this study. To directly compare the concentration in precipitation, a comparison of the volume-weighted mean concentrations of NO_3^- and NH_4^+ in precipitation was performed. This comparison showed that the NMB for the volume-weighted mean concentration in precipitation was around −30%, which was higher than for wet deposition (Supplementary Information). The underestimation of precipitation can be partly attributed to the underestimation of the wet deposition (Fig. 4(g)). Precipitation is an important factor to calculate the wet deposition, and precipitation adjustment can be used to improve the estimation of wet deposition (Zhang et al., 2018; Itahashi et al., 2020a); however, such adjustment does not consider the budget for air pollutants, and this method was not used in

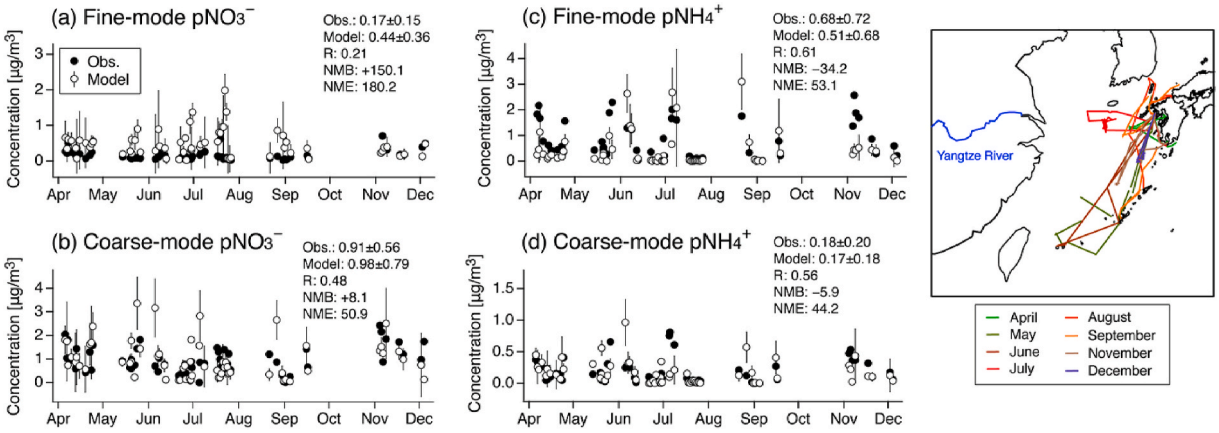

Fig. 5. Temporal variations of observations by the ship Nagasaki Maru (black circles) and model simulations (white circles) in the nested domain for ambient concentrations of (a) fine-mode pNO_3^-, (b) coarse-mode pNO_3^-, (c) fine-mode pNH_4^+, and (d) coarse-mode pNH_4^+. A total of 62 datasets were used. The model results are shown as average concentrations along the ship track and the standard deviations are indicated by whiskers. The map shows all ship tracks, with different colors denoting months in 2010.

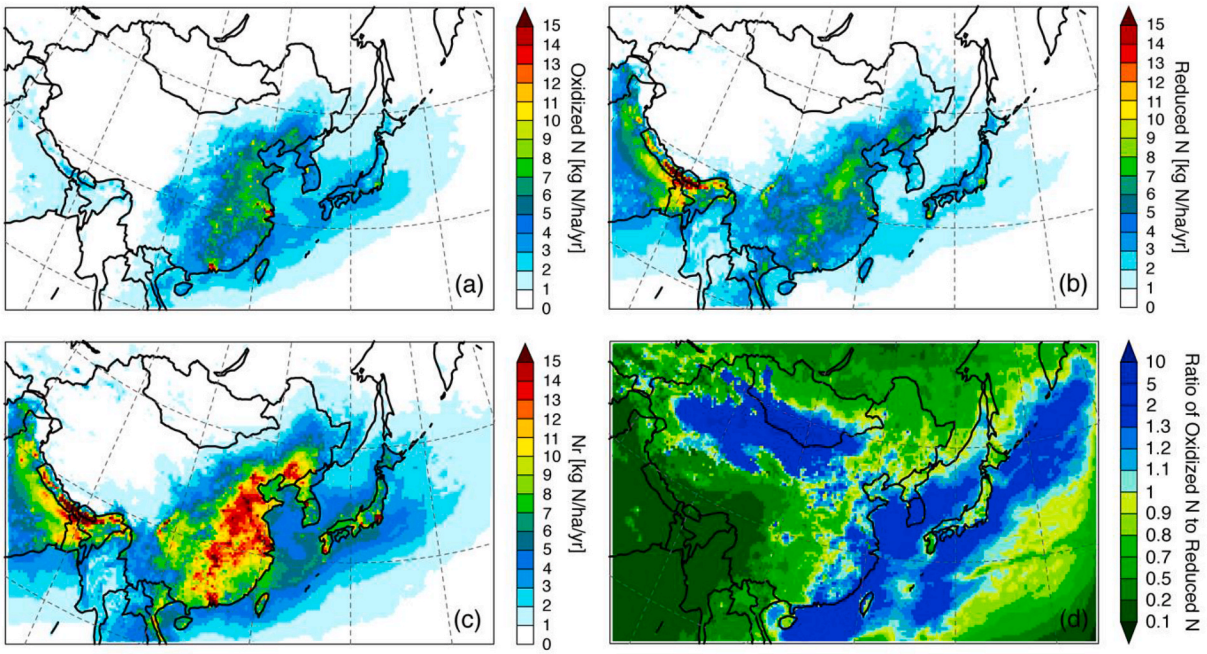

Fig. 6. Spatial distribution of the simulated total deposition (sum of dry and wet deposition) of (a) oxidized N, (b) reduced N, (c) Nr, and (d) the ratio of oxidized N to reduced N over East Asia. Values greater than unity (blue colors) indicate an oxidized-N-rich status and values less than unity (green colors) indicate a reduced-N-rich status.

this study. The modeling performance for wet deposition achieved in this work was comparable to that reported in MICS-Asia (Itahashi et al., 2020a; Ge et al., 2020). It is notable that wet deposition in East Asia was markedly higher. For example, the value of 10 kg N ha^{-1} yr^{-1} has been proposed for diagnosing the threat of N deposition for biodiversity on land (Bleeker et al., 2011), that is, an average of 0.83 kg N/ha/month. Some sites in East Asia located near coastline exceeded this value by the wet deposition of NO_3^- or NH_4^+. If these wet deposition are summed and dry deposition are also included, the N deposition over East Asia can be considered to represent a high risk to biodiversity.

3.2. Evaluation of modeling performance over the East China sea

Observations of the size-resolved aerosol in the eastern ECS obtained by the Nagasaki Maru between April and December 2010 were further used to evaluate the modeling performance. The ship tracks and the temporal variations of the size-resolved aerosol concentration are shown in Fig. 5. Overall, the model simulation in the nested domain accurately captured the temporal variation of the size-resolved pNO_3^- and pNH_4^+ along the ship tracks; however, the model performed poorly for fine-mode pNO_3^-, especially in summer. The observed concentrations were close to 0 μg m^{-3}, whereas the model sometimes simulated concentrations greater than 1 μg m^{-3}, leading to large values of NMB and NME. These values were mainly obtained in the sea south of Jeju Island in the Republic of Korea, and the model simulated the outflow from the Asian continent to the ECS. In a previous study, measurements from research vessels in the western ECS during 2005–2007 obtained mean (±standard deviation) concentrations of pNO_3^- and pNH_4^+ of 2.4 ± 2.8 and 1.6 ± 1.4 μg m^{-3}, respectively (Hsu et al., 2010). These values are much higher than those measured by the Nagasaki Maru over the eastern ECS,

Table 2
Simulated deposition amount over marginal seas and open ocean in East Asia. The unit is Gg N yr^{-1} and values in parentheses indicate the percentage contribution to the total deposition.

	Dry deposition	Wet deposition	Total
Yellow Sea (YS)			
HNO_3	25.4 (10.9%)	0.0 (0.0%)	25.4 (10.9%)
Fine-mode NO_3^-	3.0 (1.3%)	**30.8 (13.3%)**	33.8 (14.6%)
Coarse-mode NO_3^-	**47.9 (20.6%)**	13.8 (5.9%)	61.7 (26.6%)
Other oxidized N species	4.9 (2.1%)	0.1 (0.1%)	5.1 (2.2%)
NH_3	26.7 (11.5%)	0.0 (0.0%)	26.7 (11.5%)
Fine-mode NH_4^+	3.6 (1.5%)	**39.7 (17.1%)**	43.2 (18.6%)
Coarse-mode NH_4^+	28.9 (12.4%)	7.3 (3.1%)	36.1 (15.6%)
Total	140.4 (60.5%)	91.7 (39.5%)	232.0
East China Sea (ECS)			
HNO_3	24.7 (6.3%)	0.0 (0.0%)	24.7 (6.3%)
Fine-mode NO_3^-	2.0 (0.5%)	43.9 (11.3%)	45.9 (11.8%)
Coarse-mode NO_3^-	**93.7 (24.0%)**	**49.5 (12.7%)**	143.2 (36.7%)
Other oxidized N species	5.4 (2.3%)	0.4 (0.2%)	5.8 (2.5%)
NH_3	18.1 (4.6%)	0.1 (0.0%)	18.1 (4.6%)
Fine-mode NH_4^+	3.4 (0.9%)	**86.0 (22.1%)**	89.4 (22.9%)
Coarse-mode NH_4^+	39.9 (10.2%)	22.9 (5.9%)	62.8 (16.1%)
Total	187.2 (48.0%)	202.7 (52.0%)	389.9
Sea of Japan (SJ)			
HNO_3	24.4 (6.7%)	0.0 (0.0%)	24.4 (6.7%)
Fine-mode NO_3^-	3.1 (0.9%)	**48.5 (13.4%)**	51.6 (14.3%)
Coarse-mode NO_3^-	**70.0 (19.3%)**	45.5 (12.6%)	115.5 (31.9%)
Other oxidized N species	6.6 (2.8%)	0.6 (0.3%)	7.2 (3.1%)
NH_3	25.3 (7.0%)	0.0 (0.0%)	25.3 (7.0%)
Fine-mode NH_4^+	4.8 (1.3%)	**76.0 (21.0%)**	80.8 (22.3%)
Coarse-mode NH_4^+	36.7 (10.1%)	20.4 (5.6%)	57.0 (15.8%)
Total	170.9 (47.2%)	191.0 (52.8%)	361.8
Northwest Pacific (NWP)			
HNO_3	27.7 (3.9%)	0.0 (0.0%)	27.9 (3.9%)
Fine-mode NO_3^-	1.9 (0.3%)	79.6 (11.3%)	81.5 (11.5%)
Coarse-mode NO_3^-	**163.0 (23.1%)**	**99.5 (14.1%)**	262.5 (37.1%)
Other oxidized N species	11.9 (5.1%)	1.2 (0.5%)	13.1 (5.6%)
NH_3	35.9 (5.1%)	0.1 (0.0%)	36.0 (5.1%)
Fine-mode NH_4^+	3.9 (0.6%)	**160.0 (22.6%)**	163.9 (23.2%)
Coarse-mode NH_4^+	68.7 (9.7%)	53.7 (7.6%)	122.4 (17.3%)
Total	312.9 (44.3%)	394.2 (55.7%)	707.1

Note: The top three processes for each investigated area are shown in bold font.

suggesting that the ECS is sensitive to the outflow of air pollution from the Asian continent. In addition to the evaluation with EANET, this verification of the modeled size-resolved pNO_3^- and pNH_4^+ along measurement tracks of the Nagasaki Maru increases the confidence in the estimation of the N burden over East Asia presented in this study. The estimation of the N burden over East Asia is discussed in the following section.

3.3. Estimation of nitrogen burden over East Asian oceans

The spatial distribution of the N deposition over East Asia is illustrated in Fig. 6. The total deposition (sum of dry and wet processes) of oxidized N (Fig. 6(a)) and reduced N (Fig. 6(b)) showed a similar spatial distribution, with large values over the Asian continent (especially eastern mainland China), which extended into downwind regions of Japan and the Western Pacific. For the total Nr deposition (Fig. 6(c)), most of eastern mainland China, Seoul, and some parts of Japan (e.g., Osaka, Nagoya, and Tokyo) showed a total Nr deposition of 10 kg N ha^{-1} yr^{-1} or more. The YS, ECS, and SJ showed a high N burden of 2–9 kg N ha^{-1} yr^{-1}. The regional averaged wet deposition of the sum of NO_3^- and NH_4^+ are 2.3, 2.8, 1.9, and 1.5 kg N ha^{-1} yr^{-1} over the YS, ECS, SJ, and NWP, respectively (Supplemental Information). Based on enrichment experiments, the growth of phytoplankton (e.g., *Synechococcus*) was observed within 1 day due to an increase of inorganic nitrogen of 0.6 μM (Takeda et al., 2014). Given that the mixture of our estimated wet deposition over 1 m surface depth, these are corresponded to 11–21 day supply of nutrients to lead to the activated biological process. These results demonstrate the importance of the role of the atmospheric N burden to East Asian. To investigate the role of oxidized and reduced N, their ratio is shown in Fig. 6(d). The dominance of oxidized N and reduced N over ocean and land, respectively, was closely related to the characteristics of emissions as seen from Fig. 2(c). The dominance of oxidized N was found in desert areas in north-central to western parts of China, which was due to the large dry deposition of coarse-mode pNO_3^-. Meanwhile, the dominance of reduced N was seen over open ocean far from land (bottom-right part of Fig. 6(d)), despite the emission ratio (Fig. 2(c)). This was considered to be due to the long-range transport of pNH_4^+ (as ammonium sulfate ($(NH_4)_2SO_4$); e.g., Itahashi et al., 2017). From the simulated spatial distribution of the total Nr deposition (Fig. 6(c)), a clear contrast can be seen between land and ocean, with high deposition over land and low deposition over oceans. Based on ground-based observations in coastal China during 2010–2012, the annual total deposition were estimated to range from 22.0 to 44.6 kg N ha^{-1} yr^{-1} (Luo et al., 2014). The simulation performed in the present study agreed well with these estimates, returning values greater than 15 kg N ha^{-1} yr^{-1} in Eastern China (Fig. 6(c)).

The simulated N deposition to East Asian oceans is summarized in Table 2. Among the N deposition processes, the dry deposition of HNO_3 and NH_3, coarse-mode pNO_3^- and pNH_4^+, and the wet deposition of NO_3^- and NH_4^+ were quantitatively important. The importance of the dry deposition of HNO_3 and NH_3 in the YS, which is adjacent to the Asian continent, was greater than that in the other studied oceans. Compared to marginal seas, a higher weight by wet deposition of NO_3^- and NH_4^+ was seen over the NWP. Contributions of oxidized N other than HNO_3 and NO_3^- were relatively lower, and N_2O_5 and PANs were dominant. Over the NWP, the importance of PANs was larger than over marginal seas and the contributions of other oxidized N species were higher. This is because PAN is an important reservoir of N in remote sites (Seinfeld and Pandis, 2016). Note that the estimated oxidized N deposition over East Asian oceans is similar to our previous estimate for the early 2000s (Itahashi et al., 2016). Under the increasing NO_x emissions in China up to 2011, it was expected that the N deposition would also have increased prior to this year; however, this was not found in this study. Based on a summary of the available dataset in China, the bulk N deposition showed an increasing trend from the 1980s to 2000, but no increasing trend was observed from 2000 to 2010 (Liu et al., 2013). EANET observations show that the wet deposition of NO_3^- had an almost flat trend during 2000–2015 (Itahashi et al., 2018a). Because China's SO_2 emissions have declined since 2005, this trend could be connected to the decrease of the deposition related to NH_4^+ (via $(NH_4)_2SO_4$). Elucidating the long-term trends of N burden and the balance between oxidized and reduced N is an important aspect for deposition analysis, and long-term simulations based on the unified modeling design are required in future work.

3.4. Detailed examination over the East China sea

In this section, the estimated N deposition to the ECS based on the high-resolution modeling is discussed. As shown in Fig. 6(c), the modeling suggests that the ECS received a large amount of N deposition along the Asian continent and the N deposition to the ECS showed a decreasing gradient from west to east. The annual maximal riverine exports of nitrate and ammonia from the Yangtze River to the ECS in the 1990s were estimated to be 430 and 190 Gg N yr^{-1}, respectively (Nakamura et al., 2005). Although these riverine exports have been changing due to the increase of N inputs (e.g., Wang et al., 2014) and the decline of fluvial water (e.g., Yang et al., 2015), the estimated N deposition of 390 Gg N yr^{-1} over the ECS that was obtained in this study (Table 2) demonstrates the non-negligible impact of deposition compared with river discharge. In other studies, enhanced nitrate concentration at the nutrient-depleted surface over the ECS during summer was ascribed to rainfall (Kodama et al., 2011). These patches of elevated nitrate concentration were horizontally limited to within tens of

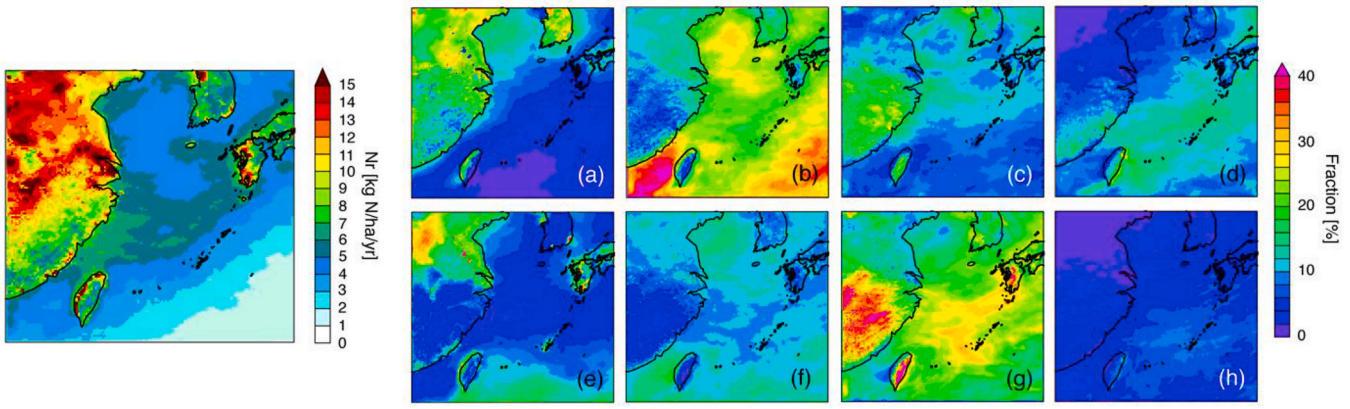

Fig. 7. Spatial distribution of the simulated Nr deposition using a high-resolution nested domain over the East China Sea and the fraction of its components shown as percentages. (a) Dry deposition of HNO_3, (b) dry deposition of coarse-mode pNO_3^-, (c) wet deposition of fine-mode NO_3^-, and (d) wet deposition of coarse-mode NO_3^- for oxidized N. (e) Dry deposition of NH_3, (f) dry deposition of coarse-mode pNH_4^+, (g) wet deposition of fine-mode NH_4^+, and (h) wet deposition of coarse-mode NH_4^+ for reduced N.

kilometers; therefore, high-resolution modeling for the ECS is important.

The estimated N deposition over the ECS and the fraction of each component are illustrated in Fig. 7. This fine-scale simulation showed a clearer trend in the large N deposition over the East China Sea and its decreasing gradient from west to east. Overall, the dry deposition of coarse-mode pNO_3^- (Fig. 7(b)) and the wet deposition of fine-mode NH_4^+ (Fig. 7(g)) were found to be the dominant processes in N deposition in the ECS (see also Table 2). The fractions of the dry deposition of the gaseous species HNO_3 (Fig. 7(a)) and NH_3 (Fig. 7(e)) were higher over land than over ocean. It is noteworthy that the wet deposition showed different contribution patterns over the ECS. The wet deposition of fine-mode NO_3^- (Fig. 7(c)) was found to be more important over the north-eastern ECS, whereas the wet deposition of coarse-mode NO_3^- (Fig. 7(d)) was found to dominate in the southern ECS. Because wet deposition is related to precipitation patterns, which vary from year to year, future research of the long-term trend of N deposition over the ECS should consider changes in human-induced emissions of Nr to the atmosphere.

4. Conclusion

The N burden into East Asian oceans via atmospheric deposition in 2010 was estimated based on a regional chemical transport model. The modeling performance was evaluated by comparison with EANET observations and data acquired by the ship Nagasaki Maru. It was found that the YS, ECS, and SJ had a high N burden of between 2 and 9 kg N ha^{-1} yr^{-1}. The most important processes for N deposition were found to be the dry deposition of HNO_3, NH_3, and coarse-mode pNO_3^-, and the wet deposition of fine-mode NO_3^- and NH_4^+. Furthermore, the relative importance of the dry deposition of coarse-mode pNO_3^- was higher over open ocean. The estimated N deposition to the whole ECS was 390 Gg N yr^{-1}, which is comparable to the discharge from the Yangtze River to the ECS, indicating the significant contribution of atmospheric deposition to the N burden. The modeled deposition of oxidized N over marginal seas in 2010 was similar to the reported values for the 2000s, despite the increase of anthropogenic emissions between these two periods. Future work should estimate the long-term variation of the compositions of oxidized and reduced N to clarify the N burden over East Asia.

The modeling performance for the ambient concentration and wet deposition remarked the criteria and was found to be comparable to previous modeling studies. However, the scores of biases and errors should be improved to refine the estimation of the ambient concentration and hence of the deposition amount. In this study, the dust scheme was incorporated to improve the modeling performance; however, heterogeneous reactions on dust surfaces were not considered. Heterogeneous reactions are thought to play an important role during dust pollution episodes (Uno et al., 2017a, 2017b; 2017c; Wang et al., 2017); therefore, the consideration of such reactions will help to refine the modeling performance. Additionally, the verification of the simulated dry deposition velocity using measurement data (Nakahara et al., 2019; Xu and Matsuda, 2020) is also required to improve the estimation of the dry deposition amount. Alongside these modeling improvements, indexes should be established for the judgement of the modeling performance over Asia, and the threshold value for assessing the risk of the N burden over Asia should be considered.

CRediT author contribution statement

Syuichi Itahashi: Conceptualization, Methodology, Validation, Formal analysis, Investigation, Writing – Original Draft, Visualization; **Kentaro Hayashi**: Conceptualization, Writing – Original Draft; **Shigenobu Takeda**: Investigation, Resources; **Yu Umezawa**: Investigation, Resources; **Kazuhide Matsuda**: Investigation, Writing – Review & Editing; **Tatsuya Sakurai**: Investigation, Writing – Review & Editing; **Itsushi Uno**: Methodology, Writing – Review & Editing.

Funding

This work was supported by MEXT/JSPS KAKENHI grant number JP18H03359.

Declaration of competing interest

The authors declare that they have no known competing financial interests or personal relationships that could have appeared to influence the work reported in this paper.

Acknowledgments

The authors are grateful to EANET for providing observational data. The authors thank marineregions.org (https://www.marineregions.org/about.php) for providing the shapefiles of the ocean areas defined by the IHO. The authors would like to thank Ms. Misato Yamada and the captains and crews of the T/S Nagasaki Maru for their help in aerosol sample collection and analysis.

Appendix A. Supplementary data

Supplementary data to this article can be found online at https://doi.org/10.1016/j.envpol.2021.117309.

References

Baker, A.R., Kanakidou, M., Altierl, K.E., Dashkalakis, N., Okin, G.S., Myriokefalitakis, S., Dntener, F., Uematsu, M., Sarin, M.M., Duce, R.A., Galloway, J.N., Keene, W.C., Singh, A., Zamora, L., Lamarque, J.-F., Hsu, S.-C., Rohekar, S.S., Prospero, J.M., 2017. Observation- and model-based estimates of particulate dry nitrogen deposition to the oceans. Atmos. Chem. Phys. 17, 8189–8210.

Ban, S., Matsuda, K., Sato, K., Ohizumi, T., 2016. Longterm assessment of nitrogen deposition at remote EANET sites in Japan. Atmos. Environ. 146, 70–78.

Bleeker, A., Hicks, W.K., Dentener, F., Galloway, J., Erisman, J.W., 2011. N deposition as a threat to the world's protected areas under the convention on biological diversity. Environ. Pollut. 159, 2280–2288. https://doi.org/10.1016/j.envpol.2010.10.036.

Chen, C.-T.A., Wang, S.-L., 1999. Carbon, alkalinity and nutrient budgets on the East China Sea. J. Geophys. Res. 106, 20675–20686.

Chen, L., Gao, Y., Zhang, M., Fu, J.S., Zhu, J., Liao, H., Li, J., Huang, K., Ge, B., Lee, H.-J., Wang, X., Lam, Y.-F., Lin, C.-Y., Itahashi, S., Nagashima, T., Kajino, M., Yamaji, K., Wang, Z., Kurokawa, J., 2019. MICS-Asia III: multi-model comparison and evaluation of aerosol over East Asia. Atmos. Chem. Phys. 19, 11911–11937.

Darmenova, K., Sokolik, I.N., Shao, Y., Marticorena, B., Bergametti, G., 2009. Development of a physically based dust emission modeule within the Weather Research and Forecasting (WRF) model: assessment of dust emission parameterizations and input parameters for source regions in Central and East Asia. J. Geophys. Res. 114, D14201.

Duce, D.A., LaRoche, J., Altieri, K., Arrigo, K.R., Baker, A.R., Capone, D.G., Cornell, S., Dentener, F., Galloway, J., Ganeshram, R.S., Geider, R.J., Jickells, T., Kuypers, M.M., Langlois, R., Liss, P.S., Liu, S.M., Middleburg, J.J., Moore, C.M., Nickovic, S., Oshchlies, A., Pedersen, T., Prospero, J., Schlitzer, R., Seitzinger, S., Sorensen, L.L., Uematsu, M., Ulloa, O., Voss, M., Ward, B., Zamoram, L., 2008. Impacts of atmospheric anthropogenic nitrogen on the open ocean. Science 320, 893–897.

EANET (Acid Deposition Monitoring Network in East Asia), 2010a. Technical Manual on Dry Deposition Flux Estimation in East Asia. http://www.eanet.asia/product/manual/techdry.pdf (accessed 4 January 2021).

EANET (Acid Deposition Monitoring Network in East Asia), 2010b. Technical Manual for Wet Deposition Monitoring in East Asia. http://www.eanet.asia/product/manual/techwet.pdf (accessed 4 January 2021).

EANET (reportAcid Deposition Monitoring Network in East Asia), 2012. Data report 2010. https://monitoring.eanet.asia/document/public/index. (accessed 4 January 2021).

EANET (Acid Deposition Monitoring Network in East Asia), 2020. http://www.eanet.asia. (Accessed 11 November 2020).

Emery, C., Liu, Z., Russell, A.G., Odman, M.T., Yarwood, G., Kumar, N., 2017. Recommendations on statistics and benchmarks to assess photochemical model performance. J. Air Waste Manag. Assoc. 67, 582–598. https://doi.org/10.1080/10962247.2016.1265027.

Emmons, L.K., Walters, S., Hess, P.G., Lamarque, J.-F., Pfister, G.G., Fillmore, D., Granier, C., Guenther, A., Kinnison, D., Laepple, T., Orlando, J., Tie, X., Tyndall, G., Wiedinmyer, C., Baughcum, S.L., Kloster, S., 2010. Description and evaluation of the model for ozone and related chemical Tracers, version 4 (MOZART-4). Geosci. Model Dev 3, 43–67.

Endo, T., Yagoh, H., Sato, K., Matsuda, K., Hayashi, K., Noguchi, I., Sawada, K., 2011. Regional characteristics of dry deposition of sulfur and nitrogen compounds at EANET sites in Japan from 2003 to 2012. Atmos. Environ. 45, 1259–1267.

Fahey, K.M., Garlton, A.G., Pye, H.O.T., Baek, J., Hutzell, W.T., Stanier, C.O., Bake, K.R., Appel, K.W., Jaoui, M., Offenberg, J.H., 2017. A framework for expanding aqueous chemistry in the Community Multiscale Air Quality (CMAQ) model version 5.1. Geosci. Model Dev 10, 1057–1605.

Foroutan, H., Young, J., Napelenok, S., Ran, L., Appel, K.W., Gilliam, R.C., Pleim, J.E., 2017. Development and evaluation of a physics-based windblown dust emission scheme implemented in the CMAQ modeling system. J. Adv. Model. Earth Syst. 9, 585–608.

Fowler, D., Coyle, M., Skiba, U., Suttom, M.A., Cape, N., Reis, S., Sheppard, L.J., Jenkins, A., Grizzertti, B., Galloway, J.N., Vitousek, P., Leach, A., Bouwman, A.F., Butterbach-Bahl, K., Dentener, F., Stevenson, D., Amann, M., Voss, M., 2013. The global nitrogen cycle in the twenty-first century. Phil. Trans. R. Soc. B 368, 20130164.

Galmarini, S., Koffi, B., Solazzo, E., Keating, T., Hogrefe, C., Schulz, M., Benedictow, A., Griesfeller, J.J., Janssens-Maenhout, G., Carmichael, G., Fu, J., Dentener, F., 2017. Technical note: coordination and harmonization of the multi-scale multi-model activities HTAP2, AQMEII3, and MICS-Asia 3: simulations, emission inventories, boundary conditions, and model output formats. Atmos. Chem. Phys. 17, 1543–1555.

Galloway, J.N., Dentener, F.J., Capone, D.G., Boyer, E.W., Howarth, R.W., Seitzinger, S.P., Asner, G.P., Cleveland, C.C., Green, P.A., Holland, E.A., Karl, D.M., Michaels, A.F., Porter, J.H., Townsend, A.R., Vorosmarty, C.J., 2004. Nitrogen cycles: past, present, and future. Biogeochemistry 70, 153–226.

Gantt, B., Kelly, J.T., Bash, J.O., 2015. Updating sea spray aerosol emissions in the Community Multiscale Air Quality (CMAQ) model version 5.0.2. Geosci. Model Dev. (GMD) 8, 3733–3746.

Gesamp (Imo/Fao/Unesco-Ioc/Unido/Wmo/Iaea/Un/Un Environment/Undp Joint Group of Experts on the Scientific Aspects of Marine Environmental Protection), 2018. The magnitude and impacts of anthropogenic atmospheric nitrogen inputs to the ocean. Rep. Stud. GESAMP 47. No. 97/GAW Report No. 238.

Ge, B., Itahashi, S., Sato, K., Xu, D., Wang, J., Fan, F., Tan, Q., Fu, J.S., Wang, X., Yamaji, K., Nagashima, T., Li, J., Kajino, M., Liao, H., Zhang, M.G., Wang, Z., Li, M., Woo, J.-H., Kurokawa, J., Pan, Y., Wu, Q., Liu, X., Wang, Z.F., 2020. Model inter-comparison study for Asia (MICS-Asia) phase III: multimodel comparison of reactive nitrogen deposition over China. Atmos. Chem. Phys. 20, 10587–10610.

Gonzales, A.T., Kelley, E., Bernad, S.R.Q., 2019. A review of intergovernmental collaboration in ecosystem-based governance of the large marine ecosystems of East Asia. Deep-Sea Res. Pt. II 163, 108–119.

Guenther, A.B., Jiang, X., Heald, C.L., Sakulyanontvittaya, T., Duhl, T., Emmons, L.K., Wang, X., 2012. The Model of Emissions of Gases and Aerosols from Nature version 2.1 (MEGAN2.1). An extended and updated framework for modeling biogenic emissions. Geosci. Model Dev. (GMD) 5, 1471–1492.

Hsu, S.-C., Wong, G.T.F., Gong, G.-C., Shiah, F.-K., Huang, Y.-T., Kao, S.-J., Tsai, F., Lung, S.-C.C., Lin, F.-J., Lin, I.-I., Hung, C.-C., Tseng, C.-M., 2010. Sources, solubility, and dry deposition of aerosol trace elements over the East China Sea. Mar. Chem. 120, 116–127.

Hutzell, W.T., Luecken, D.J., Appel, W.K., Carter, W.P., 2011. Interpreting predictions from the SAPRC07 mechanism based on regional and continental simulations. Atmos. Environ. 46, 417–429.

INMS (International Nitrogen Management System), 2020. Updated Outline for the International Nitrogen Assessment. NWG Briefing-1/Inf.Doc.1, Implementation of the UNEA-4 Resolution on Sustainable Nitrogen Management (UNEP/EA.4/Res.14).

INMS, 2021. Towards the Establishment of International Nitrogen Management System (INMS). https://www.inms.international/(accessed 14 January 2021).

IOC-UNESCO (Intergovernmental Oceanographic Commission of UNESCO), UNEP (United Nations Environment Programme), 2016. Large Marine Ecosystems: Status and Trends. UNEP, Nairobi, Kenya.

Itahashi, S., Uno, I., Irie, H., Kurokawa, J., Ohara, T., 2014. Regional modeling of tropospheric NO_2 vertical column density over East Asia during the period 2000–2010: comparison with multisatellite observations. Atmos. Chem. Phys. 14, 3623–3635.

Itahashi, S., Uno, I., Hayami, H., Fujita, S., 2015. Variation of the ratio of nitrate to non-seasalt sulfate in precipitation over East Asia with emissions from China. Atmos. Environ. 118, 87–97.

Itahashi, S., Hayami, H., Uno, I., Pan, X., Uematsu, M., 2016. Importance of coarse-mode nitrate produced via sea-salt as atmospheric input to East Asian oceans. Geophys. Res. Lett. 43, 5483–5491.

Itahashi, S., Uno, I., Osada, K., Kamiguchi, Y., Yamamoto, S., Tamura, K., Wang, Z., Kurosaki, Y., Kanaya, Y., 2017. Nitrate transboundary heavy pollution over East Asia in winter. Atmos. Chem. Phys. 17, 3823–3843.

Itahashi, S., Yumimoto, K., Uno, I., Hayami, H., Fujita, S.-I., Pan, Y., Wang, Y., 2018a. A 15-year record (2001–2015) of the ratio of nitrate to non-sea-salt sulfate in precipitation over East Asia. Atmos. Chem. Phys. 18, 2835–2852.

Itahashi, S., Yamaji, K., Chatani, S., Hayami, H., 2018b. Refinement of modeled aqueous-phase sulfate production via the Fe- and Mn-catalyzed oxidation pathway. Atmosphere 9, 132.

Itahashi, S., Yamaji, K., Chatani, S., Hisatsune, K., Saito, S., Hayami, H., 2018c. Model performance differences in sulfate aerosol in winter over Japan based on regional chemical transport models of CMAQ and CAMx. Atmosphere 9, 488.

Itahashi, S., Yumimoto, K., Kurokawa, J., Morino, Y., Nagashima, T., Miyazaki, K., Maki, T., Ohara, T., 2019. Inverse estimation of NOx emissions over China and India 2005-2016: contrasting recent trends and future perspectives. Environ. Res. Lett. 14, 124020. https://doi.org/10.1088/1748-9326/ab4d7f.

Itahashi, S., Ge, B.Z., Sato, K., Fu, J.S., Wang, X.M., Yamaji, K., Nagashima, T., Li, J., Kajino, M., Liao, H., Zhang, M.G., Wang, Z., Li, M., Kurokawa, J., Carmichae, G.R., Wang, Z.F., 2020a. MICS-Asia III: overview of model intercomparison and evaluation of acid deposition over Asia. Atmos. Chem. Phys. 20, 2667–2693.

Itahashi, S., Mathur, R., Hogrefe, C., Zhang, Y., 2020b. Modeling stratospheric intrusion and trans-Pacific transport on tropospheric ozone using hemispheric CMAQ during April 2010–Part 1: model evaluation and air mass characterization for stratosphere–troposphere transport. Atmos. Chem. Phys. 20, 3373–3396.

Irie, H., Muto, T., Itahashi, S., Kurokawa, J., Uno, I., 2016. Turnaround of tropospheric nitrogen dioxide pollution trends in China, Japan, and South Korea. SOLA 12, 170–174.

Janssens-Maenhout, G., Crippa, M., Guizzardi, F., Dentener, F., Muntean, M., Pouliot, G., Keating, T., Zhang, Q., Kurokawa, J., Wankmuller, R., Danier van der Gon, H., Kuenen, J.J.P., Kilmont, Z., Frost, G., Darras, S., Koffi, B., Li, M., 2015. HTAP_v2.2: a mosaic of regional and global emission grid maps for 2008 and 2010 to study hemispheric transport of air pollution. Atmos. Chem. Phys. 15, 11411–11432.

JELA (Japan Environmental Laboratories Association), 2020. (in Japanese). http://db.cger.nies.go.jp/dataset/acidrain/ja/(accessed 1 December 2020).

Jickells, T.D., Buitenhuis, E., Altieri, K., Baker, A.R., Capone, D., Duce, R.A., Dentener, F., Fennel, K., Kanakidou, M., LaRoche, J., Lee, K., Liss, P., Middelburg, J.J., Moore, J. K., Okin, G., Oschlies, A., Sarin, M., Seitzinger, S., Sharples, J., Singh, A., Suntharalingam, P., Uematsu, M., Zamora, L.M., 2016. A reevaluation of the magnitude and impacts of anthropogenic atmospheric nitrogen inputs on the ocean. Global Biogeochem. Cycles 31, 289–305. https://doi.org/10.1002/2016GB005586.

JMA (Japan Meteorological Agency), 2020. (in Japanese). http://www.data.jma.go.jp/svd/vois/data/tokyo/volcano.html (accessed 1 November 2020).

Karydis, V.A., Tsimpodi, A.P., Pozzer, A., Astitha, M., Lelieveld, J., 2016. Effects of mineral dust on global atmospheric nitrate concentrations. Atmos. Chem. Phys. 16, 1491–1509.

Kim, T.-W., Lee, K., Najjar, R.G., Jeong, H.-D., Jeong, H.J., 2011. Increasing N abundance in the Northwestern Pacific Ocean due to atmospheric nitrogen deposition. Science 334, 505–509.

Kim, T.W., Lee, K., Duce, R., Liss, P., 2014. Impact of atmospheric nitrogen deposition on phytoplankton productivity in the South China Sea. Geophys. Res. Lett. 41, 3156–3162. https://doi.org/10.1002/2014gl059665.

Kurokawa, J., Ohara, T., 2020. Long-term historical trends in air pollutant emissions of in Asia: regional Emission inventory in ASia (REAS) version 3. Atmos. Chem. Phys. 20, 12761–12793.
Kurokawa, J., Ohara, T., Morikawa, T., Hanayama, S., Greet, J.-M., Fukui, F., Kawashima, K., Akimoto, H., 2013. Emissions of air pollutants and greenhouse gases over Asian regions during 2000–2008: regional Emission inventory in ASia (REAS) version 2. Atmos. Chem. Phys. 13, 11019–11058.
Kodama, T., Furuya, K., Hashihama, F., Takeda, S., Kanda, J., 2011. Occurrence of rain-origin nitrate patches at the nutrient-depleted surface in the East China Sea and the Philippine Sea during summer. J. Geophys. Res. 116, C08003.
Kong, L., Tang, X., Zhu, J., Wang, Z., Fu, J.S., Wang, X., Itahashi, S., Yamaji, K., Nagashima, T., Lee, H.-J., Kim, C.-H., Lin, C.-Y., Chen, L., Zhang, M., Tao, Z., Li, J., Kajino, M., Liao, H., Sudo, K., Wang, Y., Pan, Y.-P., Tang, G., Li, M., Wu, Q., Ge, B., Carmichael, G.R., 2020. Evaluation and uncertainty investigation of the NO_2, CO and NH_3 modeling over China under the framework of MICS-Asia III. Atmos. Chem. Phys. 20, 181–202.
Luo, X.S., Tang, A.H., Shi, K., Wu, L.H., Li, W.Q., Shi, W.Q., Shi, X.K., Erisman, J.W., Zhang, F.S., Liu, X.J., 2014. Chinese coastal seas are facing heavy atmospheric nitrogen deposition. Environ. Res. Lett. 9, 095007.
Li, M., Liu, H., Geng, G., Hong, C., Liu, F., Song, Y., Tong, D., Zheng, B., Cui, H., Man, H., Zhang, Q., He, K., 2017. Anthropogenic emission inventories in China: a review. Nat. Sci. Rev. 4, 834–866.
Liu, X.J., Zhang, Y., Han, W.X., Tang, A.H., Shen, J.L., Cui, Z.L., Vitousek, P., Erisman, J. W., Goulding, K., Christie, P., Fangmeier, A., Zhang, F.S., 2013. Enhanced nitrogen deposition over China. Nature 494, 459–462.
Mathur, R., Xing, J., Gilliam, R., Sarwar, G., Hogrefe, C., Pleim, J., Poliot, G., Roselle, S., Spero, T.L., Wong, D.C., Young, J., 2017. Extending the Community Multiscale Air Quality (CMAQ) modeling system to hemispheric scales: overview of process considerations and initial applications. Atmos. Chem. Phys. 17, 12449–12474.
Nakahara, A., Takagi, K., Sorimachi, A., Katata, G., Matsuda, K., 2019. Enhancement of dry deposition of $PM_{2.5}$ nitrate in a cool-temperate forest. Atmos. Environ. 212, 136–141.
Nakamura, T., Matsumoto, K., Uematsu, M., 2005. Chemical characteristics of aerosols transported from Asia to the East China Sea: an evaluation of anthropogenic combined nitrogen deposition in autumn Atmos. Environ. Times 39, 1749–1758.
Ohara, T., Akimoto, H., Kurokawa, J., Horii, N., Yamaji, K., Yan, X., Hayasaka, T., 2007. Asian emission inventory for anthropogenic emission sources during the period 1980–2020. Atmos. Chem. Phys. 7, 4419–4444.
Onitsuka, G., Uno, I., Yanagi, T., Yoon, J.-H., 2009. Modeling the effects of atmospheric nitrogen input on biological production in the Japan Sea. J. Oceanogr. 65, 433–438.
Pleim, J.E., Xiu, A., Finkelstein, P.L., Otte, T.L., 2001. A coupled land-surface and dry deposition model and comparison to field measurements of surface heat, moisture, and ozone fluxes. Water Air Soil Pollut. Focus 1, 243–252.
Pye, H.O.T., Luecken, D.J., Xu, L., Boyd, C.M., Ng, N.L., Baker, K., Ayres, B.A., Bash, J.O., Baumann, K., Carter, W.P.L., Edgerton, E., Fry, J.L., Hutzell, W.T., Schwede, D., Shepson, P.B., 2015. Modeling the current and future role of particulate organic nitrates in the southeastern United States. Environ. Sci. Technol. 49, 14195–14203.
Sakurai, T., Suzuki, T., Yoshioka, M., 2018. Model evaluation based on a relationship analysis between the emission and concentration of atmospheric ammonia in the Kanto region of Japan. Asian J. Atmos. Environ. 12, 59–66.
Sarwar, G., Simon, H., Bhave, P., Yarwood, G., 2012. Examining the impact of heterogeneous nitryl chloride production on air quality across the United States. Atmos. Chem. Phys. 12, 6455–6473.
Sarwar, G., Simon, H., Xing, J., Mathur, R., 2014. Importance of tropospheric $ClNO_2$ chemistry across the northern hemisphere. Geophys. Res. Lett. 41, 4050–4058.
Seinfeld, J.H., Pandis, S.N., 2016. Atmospheric Chemistry and Physics, from Air Pollution to Climate Change, third ed. John Wiley, New York.
Simon, H., Bhave, P.V., 2012. Simulating the degree of oxidation in atmospheric organic particles. Environ. Sci. Technol. 46, 331–339.
Shiozaki, T., Furuya, K., Kodama, T., Kitajima, S., Takeda, S., Takemura, T., Kanda, J., 2010. New estimation of N_2 fixation in the western and central Pacific Ocean and its marginal seas. Global Biogeochem. Cycles 24, GB1015.
Skamarock, W.C., Klemp, J.B., Dudhia, J., Gill, D.D., Barker, D.M., Duda, M.G., Huang, X-Y., Wang, W., Powers, J.G., 2008. A Description of the Advanced Research WRF Version 3. NCAR, Boulder, CO. NCAR Technical Note, NCAR/TN-475CSTR, p. 113.
Takeda, S., Obata, H., Okubo, A., Sato, M., Kondo, Y., 2014. Bioavailability and biogeochemical processes of trace metals in the surface ocean. TERRAPUB 163–176. https://doi.org/10.5047/w-pass.a03.001.
Taketani, F., Aita, M., Yamaji, K., Sekiya, T., Ikeda, K., Sasaoka, K., Hashioka, T., Honda, M., Matsumoto, K., Kanaya, Y., 2018. Seasonal response of North Western Pacific marine ecosystems to deposition of atmospheric inorganic nitrogen compounds from East Asia. Sci. Rep. 8, 9324.
Tan, J.N., Fu, J.S., Carmichael, G.R., Itahashi, S., Tao, Z.N., Huang, K., Dong, X.Y., Yamaji, K., Nagashima, T., Wang, X.M., Liu, Y.M., Lee, H.J., Lin, C.Y., Ge, B.Z., Kajino, M., Zhu, J., Zhang, M.G., Liao, H., Wang, Z.F., 2020. Why do models perform differently on particulate matter over East Asia? A multi-model intercomparison study for MICS-Asia III. Atmos. Chem. Phys. 20, 7393–7410.
Uematsu, M., Wang, Z., Uno, I., 2003. Atmospheric input of mineral dust to the western North Pacific region based on direct measurements and a regional chemical transport model. Geophys. Res. Lett. 30, 1342.
Uno, I., Uematsu, M., Hara, Y., He, Y.-J., Ohara, T., Mori, A., Kamaya, T., Murano, K., Sadanaga, Y., Bandow, H., 2007. Numerical study of the atmospheric input of anthropogenic total nitrate to the marginal seas in the western North Pacific region. Geophys. Res. Lett. 34, L17817.
Uno, I., Osada, K., Yumimoto, K., Wang, Z., Itahashi, S., Pan, X., Yamamoto, S., Nishizawa, T., 2017a. Seasonal variation of fine- and coarse-mode nitrates and related aerosols over East Asia: synergetic observations and chemical transport model analysis. Atmos. Chem. Phys. 17, 14181–14197.
Uno, I., Osada, K., Yumimoto, K., Wang, Z., Itahashi, S., Pan, X., Yamamoto, S., Nishizawa, T., 2017b. Importance of long-range nitrate transport based on the long-term observation and modeling of dust and pollutants over East Asia. Aerosol Air Qual. Res. 17, 3052–3064.
Uno, I., Yumimoto, K., Pan, X., Wang, Z., Osada, K., Itahashi, S., Yamamoto, S., 2017c. Simultaneous dust and pollutant transport over East Asia: the tripartite Environment Ministers meeting March 2014 case study. SOLA 13, 47–52.
Uno, I., Wang, Z., Itahashi, S., Yumimoto, K., Yamamura, Y., Yoshino, A., Takami, A., Hayasaki, M., Kim, B.-G., 2020. Paradigm shift in aerosol chemical composition over regions downwind of China. Sci. Rep. 10, 6450.
U.S. EPA (Environmental Protection Agency), 2018). CMAQ (Version 5.2.1). https://doi.org/10.5281/zenodo.1212601 (accessed 30 January 2021).
van der Werf, G.R., Randerson, J.T., Giglio, L., van Leeuwen, T.T., Chen, Y., Rogers, B.M., Mu, M., van Marle, M.J.E., Morton, D.C., Collatz, G.J., Yokelson, R.J., Kasibhatla, P. S., 2017. Global fire emissions estimates during 1997–2016. Earth Syst. Sci. Data 9, 697–720.
Wang, Q., Koshikawa, H., Liu, C., Otsubo, K., 2014. 30-year changes in the nitrogen inputs to the Yangtze River Basin. Environ. Res. Lett. 9, 115005.
Wang, Z., Itahashi, S., Uno, I., Pan, X., Osada, K., Yamamoto, S., Nishizawa, T., Tamura, K., Wang, Z., 2017. Modeling the long-range transport of particulate matters for January in East Asia using NAQPMS and CMAQ. Aerosol Air Qual. Res. 17, 3065–3078.
Wang, Z., Uno, I., Osada, K., Itahashi, S., Yumimoto, K., Chen, X., Yang, W., Wang, Z., 2020. Spatio-temporal variations of atmospheric NH_3 over East Asia by comparison of chemical transport model results, satellite retrievals and surface observations. Atmosphere 11, 900.
Xu, M., Matsuda, K., 2020. Dry deposition of $PM_{2.5}$ nitrate in a forrest according to vertical profile measurement. Asian J. Atmos. Environ. 14, 367–377.
Yamada, M., Takeda, S., Tamura, K., Shiota, Y., Yoshimura, H., 2013. Nutrient supply fluxes from atmosphere to ocean at the eastern East China Sea. Bulletin of the Faculty of Fisheries, Nagasaki University. No. 94, p.1–7 (In Japanese with English abstract and figures).
Yamaji, K., Chatani, S., Itahashi, S., Saito, M., Takigawa, M., Morikawa, T., Kanda, I., Miya, Y., Komatsu, H., Sakurai, T., Morino, Y., Kitayama, K., Nagashima, T., Shimadera, H., Uranishi, K., Fujiwara, Y., Hashimoto, T., Sudo, K., Misaki, T., Hayami, H., 2020. Model inter-comparison for $PM_{2.5}$ components over urban areas in Japan in the J-STREAM framework. Atmosphere 11, 222.
Yang, S.L., Xu, K.H., Milliman, J.D., Yang, H.F., Wu, C.S., 2015. Decline of Yangtze River water and sediment discharge: impact from natural and anthropogenic changes. Sci. Rep. 5, 12581.
Zhang, J., Guo, X., Shao, L., 2019. Tracing external sources of nutrients in the East China Sea and evaluating their contributions to primary production. Prog. Oceanogr. 176, 102122.
Zhang, J., Lui, M.G., 1994. Observations on nutrient elements and sulphate in atmospheric wet depositions over the northwest Pacific coastal oceans—Yellow Sea. Mar. Chem. 47, 173–189.
Zhang, J., Liu, S.M., Ren, J.L., Wu, Y., Zhang, G.L., 2007. Nutrient gradients from the eutrophic changjiang (Yangtze River) estuary to the oligotrophic Kuroshio waters and re-evaluation of budgets for the east China sea shelf. Prog. Oceanogr. 74, 449–478.
Zhang, Y., Mathur, R., Bash, J.O., Hogrefe, C., Xing, J., Roselle, S.J., 2018. Long-term trends in total inorganic nitrogen and sulfur deposition in the US from 1990 to 2010. Atmos. Chem. Phys. 18, 9091–9106.